Chapter 2

Theoretical Background And Experimental Methods

2.1 Introduction:

To explain the behaviour of liquid crystalline phases many theories were proposed and described in many books, some of which are listed in the references [1-6]. One of the theories is molecular field approximation. Most acceptable and widely used theories based on molecular field approximation are given by Maier-Saupe [7] for nematics and McMillan [8] for smectic A. I am describing these two theories in brief, as I have compared the experimental values with the theoretical ones obtained from these theories.

2.2 Theories of Liquid Crystalline Phases:

2.2.1 Maier-Saupe mean field theory of nematic phase of rod like molecules:

Maier and Saupe have given a molecular statistical theory of the nematic phase (N) and nematic to isotropic (N-I) phase transition. The stability of the nematic liquid crystal phase arises from the existence of the anisotropic part of the dispersion interaction energy between the molecules. This energy originates from the intermolecular electrostatic interaction. Maier and Saupe approximated the electrostatic interaction by the first term of its multipole expansion and assumed that:

i) the influence of the permanent dipoles can be neglected as far as long range nematic order is concerned.
ii) only the effect of the induced dipole-dipole interaction need to be considered.
iii) the molecules may be considered to be cylindrically symmetric about its long axis.

iv) with respect to a given molecule the distribution of the centre of mass of the remaining molecules may be taken to be spherically symmetric.

The distribution of the molecular long axis about the director is given by an orientational distribution function f(cosθ), where θ is the angle between the director and the molecular long axis. As the molecules have no head to tail asymmetry, f(cosθ) is an even function of cosθ. Thus the orientational distribution function can be written as,

$$f(\cos\theta) = \sum_{L-even} \frac{(2L+1)}{2} < P_L(\cos\theta) > P_L(\cos\theta) \qquad \textbf{2.1}$$

where $P_L(\cos\theta)$ are the L^{th} even order Legendre polynomials, and $<P_L(\cos\theta)>$ are the statistical average given by

$$< P_L(\cos\theta) >= \int_0^1 P_L(\cos\theta) f(\cos\theta) d(\cos\theta) \qquad \textbf{2.2}$$

$<P_L>$ are defined as the orientational order parameters. Humphries et al [9] has given a more comprehensive concept by including higher order terms in the mean field potential for cylindrically symmetric molecules as,

$$V(\cos\theta) = \sum_{L-even} U_L < P_L > P_L(\cos\theta) \qquad (L\neq 0) \quad \textbf{2.3}$$

where U_L are the functions of distance between the central molecule and its neighbours only. Putting Legendre polynomials, L = 2 in equation 2.2 we get,

$$< P_2(\cos\theta) >= \int_0^1 P_2(\cos\theta) f(\cos\theta) d(\cos\theta) \qquad \textbf{2.4}$$

$<P_2>$ is called the order parameter of second order. For isotropic liquid $<P_2>$ = 0 and for perfectly ordered sample $<P_2>$ =1.

Retaining the first term of the right hand side of equation 2.3, the expression for the potential energy of a single molecule can be written as

$$V(\cos\theta) = -vP_2(\cos\theta) < P_2 > \qquad \textbf{2.5}$$

where $v = -U_2$

The orientational distribution function for a single molecule is given by

$$f(\cos\theta) = Z^{-1} \exp[\, -V(\cos\theta) / kT\,] \qquad \textbf{2.6}$$

where Z is the single molecule partition function given by

$$Z = \int_0^1 \exp[\, -V(\cos\theta) / kT\,] d(\cos\theta) \qquad \textbf{2.7}$$

and k is the Boltzmann's constant.

Substituting the value of V(cosθ) and f(cosθ) from equation 2.5 and equation 2.6 into equation 2.4 we can write

$$< P_2(\cos\theta) >= \frac{\int_0^1 P_2(\cos\theta) \exp[\, P_2(\cos\theta) < P_2 > / T^*] d(\cos\theta)}{\int_0^1 \exp[\, P_2(\cos\theta) < P_2 > / T^*] d(\cos\theta)} \qquad \textbf{2.8}$$

where $T^* = kT / v$ and equation 2.8 is a self-consistent equation. For every temperature T^* we can obtain the value of $<P_2>$ that satisfies the self-consistent equation. For normal liquids corresponding to the isotropic state, the value of $<P_2> = 0$ is a solution at all temperatures. In addition, for temperatures $T^* < 0.22284$, two more solutions of $<P_2>$ appear. It has been found that the nematic phase with $<P_2> > 0$ is stable when the T^* satisfies the condition $0 \leq T^* \leq 0.22019$. When $T^* > 0.22019$, we have a stable isotropic phase with $<P_2> = 0$.

The order parameter $<P_2>$ decreases from unity to a minimum value of 0.4289 at $T^*=0.22019$. The nematic - isotropic phase transition takes place at $T^*=0.22019$ and it is of first order, as a discontinuous change of order parameter $<P_2>$ from 0.4289 to 0 occurs.

2.2.2 McMillan's theory for smectic phase:

In smectic A phase, there is a periodic density variation along the layer normal (say, z-direction) in addition to the orientational distribution of the molecular axes. McMillan proposed a simple and elegant description of smectic A liquid crystal by extending the Maier-Saupe theory to include an additional order parameter for characterizing the one-dimensional translational periodicity of a layered structure. Therefore, the single molecule distribution function can be written as:

$$\mathbf{f}(\cos\theta, z) = \sum_{\mathbf{L-even}} \sum_{\mathbf{n}} \mathbf{A}_{\mathbf{L,n}} \mathbf{P}_{\mathbf{L}}(\cos\theta)\cos\left(\frac{2\pi \mathbf{nz}}{\mathbf{d}}\right) \qquad \mathbf{2.9}$$

where d is the layer thickness. McMillan [8,10] following Kobayashi [11,12] expressed the pair potential as

$$V_M(\cos\theta, z) = -v[\delta\alpha\tau \cos\left(\frac{2\pi z}{d}\right) + \{\eta + \alpha\delta \cos\left(\frac{2\pi z}{d}\right)\} P_2(\cos\theta) \qquad \mathbf{2.10}$$

where v and δ are constants characterizing the strengths of the anisotropic and isotropic parts of interaction respectively. Here

orientational order parameter $\eta =< \mathbf{P}_2(\cos\theta) >$,

translational order parameter $\tau =< \cos\left(\frac{2\pi \mathbf{z}}{\mathbf{d}}\right) >$ and

mixed order parameter $\sigma =< \mathbf{P}_2(\cos\theta)\cos\left(\frac{2\pi \mathbf{z}}{\mathbf{d}}\right) >$

The distribution function can thus be written as

$$f_M(\cos\theta, z) = Z^{-1} \exp[\, -V_M(\cos\theta, z) / kT\,] \qquad \mathbf{2.11}$$

where Z is the single molecule partition function given by

$$Z = \int_0^1 \int_0^d \exp[\, -V_1(\cos\theta, z) / kT\,] d(\cos\theta) dz \qquad \mathbf{2.12}$$

$$\left.\begin{aligned}
\eta &= \int_0^1 \int_0^d P_2(\cos\theta) f_1(\cos\theta, z) d(\cos\theta) dz \\
\tau &= \int_0^1 \int_0^d \cos\left(\frac{2\pi z}{d}\right) f_1(\cos\theta, z) d(\cos\theta) dz \\
\sigma &= \int_0^1 \int_0^d P_2(\cos\theta) \cos\left(\frac{2\pi z}{d}\right) f_1(\cos\theta, z) d(\cos\theta) dz
\end{aligned}\right\} \quad \textbf{2.13}$$

Once again, three self-consistent equations containing η, τ and σ can be written and solved iteratively. Depending on the values of the coupling parameters, the following three possible solutions are

i) $\eta = \tau = \sigma = 0$, this describes the isotropic liquid or disordered phase;

ii) $\eta \neq 0$, $\tau = \sigma = 0$, orientational order characteristic of the nematic phase in accordance with the Maier Saupe theory;

iii) $\eta \neq 0$, $\tau \neq 0$, $\sigma \neq 0$, orientational and translational order characteristic of the smectic A phase.

For $\alpha > 0.98$, the smectic A phase transforms directly into the isotropic phase, while for $\alpha < 0.98$ there is a smectic A-nematic transition followed by a nematic-isotropic transition at higher temperature. Although nematic-isotropic transition temperature is always first order according to McMillan theory, the smectic A-nematic transition can be either first order or second order. For $T_{SN} / T_{NI} < 0.87$, the smectic A - nematic transition is second order while for $T_{SN} / T_{NI} > 0.87$, the smectic A - nematic transition is first order. T_{SN} and T_{NI} are the smectic A - nematic and nematic - isotropic transition temperature respectively.

2.3 Texture studies:

Wide variety of visual patterns are displayed by liquid crystalline substances when viewed under polarized light. These patterns are called textures, which are entirely due to the defects in structure that occurs in the long-range molecular ordering of the liquid crystalline materials. Observation of textures is one of the most important techniques for the identification and determination of transition temperatures of liquid crystalline phases. They are observed in thin layers about 10-20μm placed in between a glass slide and a cover slip. Change in textures at particular temperature indicate occurrence of phase transition. Classification of different liquid crystalline phases by the observation of textures alone is often ambiguous, and other methods are needed to support it. Detailed description of various textures, with photographs, is given by Demus and Richter [13]

2.4 X - ray diffraction from mesophases:

The structure and hence the properties of the liquid crystalline compound can best be understood from the x-ray diffraction studies of the liquid crystal compounds. Although a number of review articles are available in this field, Vainshtein [14-15] and Leadbetter [16] have given the theoretical interpretation. From x-ray experiment, the Fourier image of the correlation density function can be determined, the reconstruction of which from the scattered data yields information both on the mutual arrangement of molecules in a liquid crystal and the specific features of the orientational and translational order.

The general formula for the intensity of scattering from a system of molecules is

$$\mathbf{I(S)} = \sum_k \sum_l \sum_m \sum_n \left\langle f_{km}(\mathbf{S})\, f_{ln}^{*}(\mathbf{S}) \exp\left[i\mathbf{S}.(r_k - r_l)\right] \exp\left[\, i\mathbf{S}.(R_{ln} - R_{km})\right]\right\rangle \quad \mathbf{2.14}$$

where the brackets indicate an average over all the molecules involved. $\mathbf{r}_k$ is the centre of mass of the k^{th} molecule , f_{km} is the atomic scattering factor of the m^{th} atom in the k^{th} molecule and R_{km} is the position of the m^{th} atom in the k^{th} molecule. The scattering vector is given by $\mathbf{S} = \mathbf{K}_s - \mathbf{K}_i$, where $\mathbf{K}_s$ and $\mathbf{K}_i$ are the scattered and incident wave vectors.

For elastic scattering $|\mathbf{K}_s| = |\mathbf{K}_s| = 2\pi/\lambda$, the intensity can be written as,

$$I(S) = I_m(S) + D(S)$$

$I_m(S)$ is the molecular structure factor and D(S) is called the interference function.

$$\mathbf{I}_m(\mathbf{S}) = \sum_k \left\langle \sum_{m,n} f_{km}(\mathbf{S})\, f_{ln}^{*}(\mathbf{S}) \exp\left[\, i\mathbf{S}.(R_{ln} - R_{km})\right]\right\rangle$$

$$= \mathbf{N}\left\langle \left| \sum_m f_{kn} \exp\left(-i\mathbf{S}.R_{km}\right)\right|^2 \right\rangle$$

$$\mathbf{D(S)} = \left\langle \sum_k^m \exp\left(\, iS.r_{kl}\right) \sum_{m,n} \left\langle f_{km}(\mathbf{S})\, f_{ln}^{*}(\mathbf{S}) \exp\left[\, i\mathbf{S}.(R_{ln} - R_{km})\right]\right\rangle \right\rangle \qquad \mathbf{2.15}$$

$$\mathbf{r}_{kl} = \mathbf{r}_k - \mathbf{r}_l$$

The term $I_m(S)$ gives the scattered intensity which would be observed from a random distribution of identical molecules. D(S) contains information regarding : **(i)** molecular packing, **(ii)** orientational distribution function, **(iii)** order parameters P_L, **(iv)** apparent molecular length, **(v)** average lateral distance between the molecules, **(vi)** layer thickness in smectics, **(vii)** layer order parameters τ and $\langle z^2 \rangle$ in SmA, **(viii)** correlation lengths, **(ix)** tilt angle, **(x)** bond orientational order parameter and **(xii)** critical exponents.

X-ray diffraction of the unoriented nematic phase consists of a uniform halo just like that of an isotropic liquid. This is due to the fact that a nematic liquid crystal generally consists of a large number of domains, the molecules being ordered within each domain along the director **n**, but there is no preferred direction for the sample as a whole so that the diffraction pattern has symmetry of revolution around the direction of the x-ray beam. However, application of suitable magnetic or electric field can produce a 'monodomain' or 'aligned' or 'oriented' sample of liquid crystal.

The small angle x-ray diffraction pattern from a nematic liquid crystal oriented perpendicular to the direction of the incident x-ray beam is shown in the Figure 2.1(a).

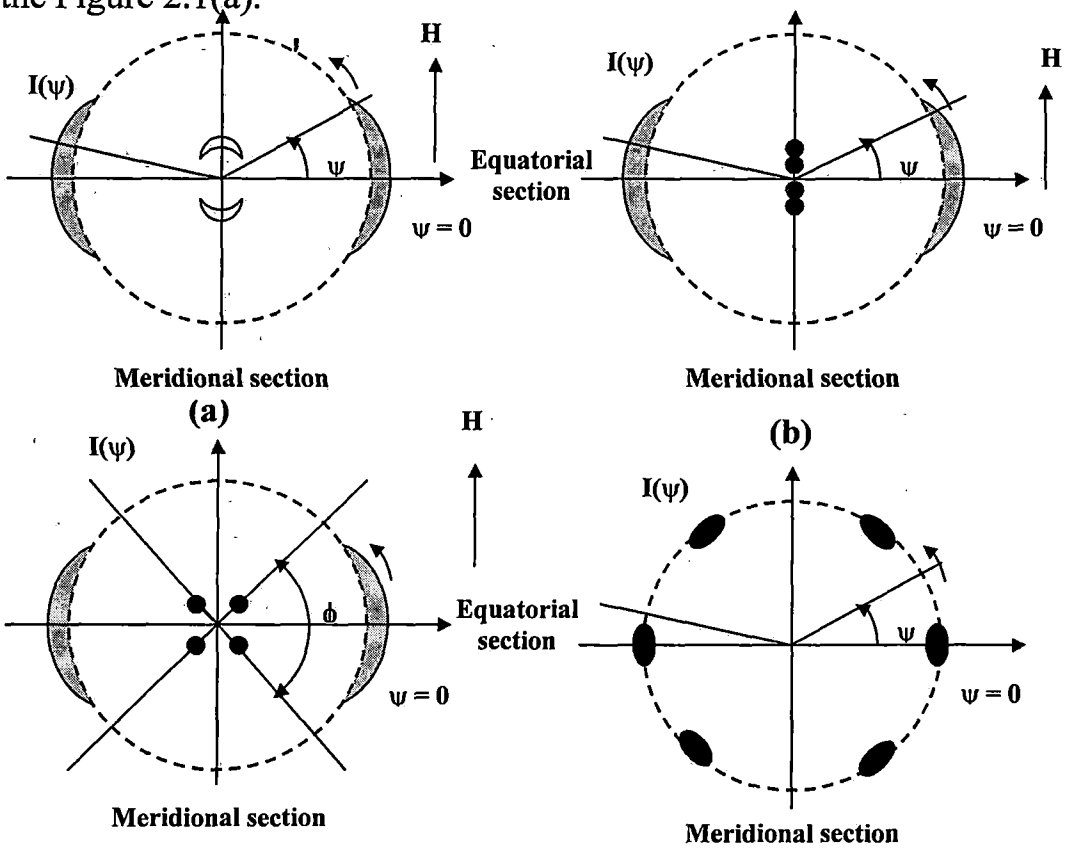

FIGURE 2.1: Schematic representation of x-ray diffraction pattern of an oriented **(a)** nematic, **(b)** smectic A, **(c)** skewed cybotactic nematic and **(d)** smectic B phase with x-ray beam parallel to the layer normal.

The outer halo splits into two crescents for each of which intensity is maxima in the equatorial direction. These crescents are formed mainly due to the intermolecular scattering and the corresponding Bragg angle is a measure of lateral intermolecular distance. The angular distribution of the x-ray intensity $I(\psi)$ vs. ψ curve, also gives the orientational distribution function $f(\cos\theta)$ and order parameter $\langle P_L \rangle$, (L= 2, 4).

At much lower scattering angle intensity peaks usually in the shape of short bar are in the meridional direction. Measuring the corresponding angle we get the value of apparent molecular length. Sometimes, the inner diffuse crescents are replaced by sharp spots (figure 2.1(c)) and the corresponding phase is called "cybotactic phase". The presence of the sharp spots indicates smectic like clusters in the nematic phase, which are called "cybotactic" groups [17].

The x-ray diffraction pattern of smectic A phase is shown in Figure 2.1(b). The meridional spots are formed due to Bragg reflection from the layers and provide the value of layer thickness. Since smectic A can have only quasi-long range order along its layer normal [3], the second order Bragg reflections in the meridional direction are generally very weak and are often absent in the x-ray photographs.

Figure 2.1(d) is the schematic representation of a three-dimensional ordered system with hexagonal symmetry, as in the smectic B phase, with the incident x-ray beam parallel to the layer normal. The outer diffraction ring is split up into six spots of strong intensity. The bond orientational order can be determined from the angular distribution of x-ray intensity $I(\psi)$ versus ψ.

2.5 Experimental technique and data analysis of X-ray diffraction studies:

The x-ray diffraction set up has been designed and fabricated in our laboratory by Jha and Paul [18]. The schematic representation of the whole set up is shown in Figure 2.2.

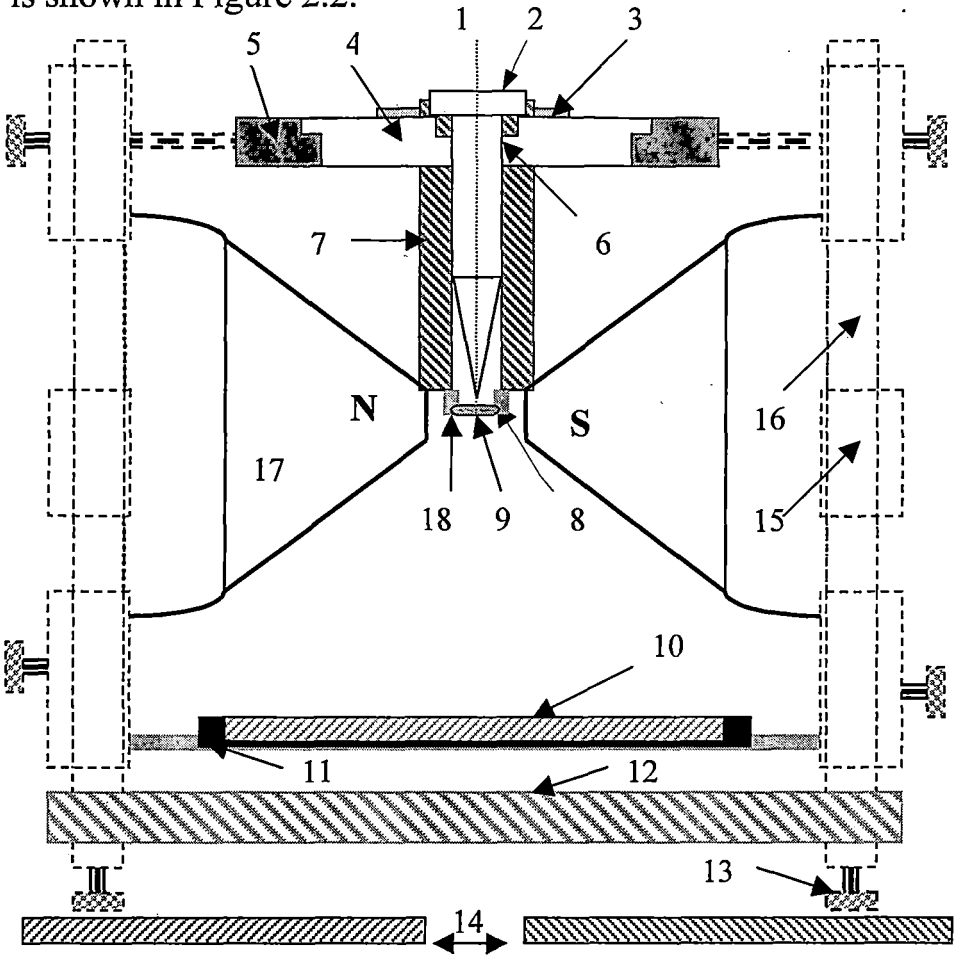

FIGURE 2.2: Sectional diagram of the X-ray diffraction camera.

1. X-ray beam, **2.** Collimator, **3.** Brass ring, **4.** Ring of syndanyo board, **5.** Brass ring, **6.** Cylindrical brass chamber, **7.** Asbestos insulation and heater winding, **8.** Specimen holder and thermocouple, **9.** Sample position, **10.** Film Cassette, **11.** Film cassette holder, **12.** Base plate, **13.** Levelling screw, **14.** Brass plates over the coils of the electromagnet, **15.** Removable spacer, **16.** Supporting brass stand, **17.** Pole pieces and **18.** Asbestos insulation.

The set up has flat-plate camera provided with the sample holder with heating arrangement. The temperature is controlled by a temperature controller of accuracy ± 0.5°C (Indotherm model IT401D2). The sample holder is fitted with a changeable collimator of aperture 0.8 mm and is well insulated. The sample was taken in a lindemann glass capillary of diameter 0.1mm and is introduced into the sample holder. The camera is then placed between the pole pieces of a strong electromagnet of field strength ~0.5 T in such a way that the sample remains at the centre of the pole pieces and the magnetic field acts along the axis of the capillary. At first the sample was heated to the isotropic phase and was slowly cooled to the desired temperature in presence of the magnetic field. X-ray photographs were taken with nickel filtered (of thickness 0.009 mm) CuK_{α} radiation of wavelength 1.5418 Å.

a) Conversion of optical density to x-ray intensity:

The optical density values obtained from the scan were then converted to relative intensity values by a method explained by Klug and Alexander [19]. The optical densities of these spots were measured with the help of photographs scanned by a Mustek 1200 UB scanner. The gray mode scan was used and the resolution was set at 600 dpi. A graph is then plotted with optical density vs. time in seconds. Since x-ray intensity is proportional to the time of exposure, the optical density vs. time curve actually corresponds to x-ray intensity and hence it is used as calibration curve to convert x-ray intensity to optical density.

b) Circular scanning of x-ray photographs:

Photographs were scanned to measure angular intensity distribution $I(\psi)$ which was used to calculate the orientational distribution function $f(\beta)$ and order parameters $< P_2>$ and $<P_4>$. Reading of the circular scan of the outer diffraction arc were taken from $\psi = 0$ to $\psi = 360^\circ$ at 1° interval near the peak and at larger intervals elsewhere. The optical density values, thus obtained, were converted into corresponding x-ray intensity with the help of the calibration curve. The experimental intensities values were then corrected for the background intensity values arising due to the air scattering. The peak intensity position which corresponds to $\psi = 0$ was determined from intensity $I(\psi)$ vs. angle (ψ) curve. $I(\psi)$ vs. ψ curve were smoothed, and nineteen values of $I(\psi)$ were taken from $\psi = 0$ to $\psi = 90^\circ$ at 5° intervals. From the values of $I(\psi)$, we have calculated the distribution function $f(\beta)$, and order parameters ($<P_2>$ and $<P_4>$) by Leadbetter's expression. A computer program was written in our laboratory for these calculations.

2.6 Orientational distribution functions and order parameters:

The x-ray diffraction pattern of an oriented sample consists of equatorial arcs. The orientational distribution function is related to the distribution of x-ray intensity along the diffused equatorial arc according to the relation given by Leadbetter and Norris [20]

$$I(\psi) = c \int_{\beta=\Psi}^{\pi/2} f_d(\beta) \sec^2 \Psi [\tan^2\beta - \tan^2\Psi]^{-1/2} \sin\beta \, d\beta \qquad \textbf{2.16}$$

where, $f_d(\beta)$ describes the distribution function of the directors of clusters in which the molecules are perfectly aligned and β is the angle between the

director **n** and molecular long axis. As molecular distribution in the nematic phase is centrosymmetric, the distribution function and the intensity can be expanded as even cosine power series.

$$I(\psi) = \sum_{n=0}^{r} a_{2n} \cos^{2n} \psi \qquad \textbf{2.17}$$

$$f_d(\beta) = \sum_{n=0}^{r} b_{2n} \cos^{2n} \beta \qquad \textbf{2.18}$$

The series converge rapidly. Retaining eight terms in the truncated series, a least square fitting was made with observed $I(\psi)$ values to get the coefficients of eqn. 2.17. These values of a_{2n} were then used to calculate the coefficients of b_{2n}.

To calculate $f_d(\beta)$ and order parameter we need $I(\psi)$ values from $\psi = 0$ to $\psi = 90^\circ$ i.e. one quadrant. I have measured $I(\psi)$ values of four quadrants separately and the average values of $I(\psi)$ is considered to calculate $f(\beta)$ as well as $\langle P_2 \rangle$ and $\langle P_4 \rangle$ for all the samples. The errors in the calculation of $\langle P_2 \rangle$ and $\langle P_4 \rangle$ in our experiment are estimated to be within $\pm$ 0.015.

$$< P_L >= \frac{\int_0^1 P_L(\cos\beta) f_d(\beta) d(\cos\beta)}{\int_0^1 f_d(\beta) d(\cos\beta)} \qquad \textbf{2.19}$$

where, L = 2,4.

2.7 Determination of Bond Orientational Order:

The order parameter associated with a system having six-fold symmetry (shown in figure 2.1(d)), as in the case of smectic B liquid crystals is the

Bond Orientational Order [21], defined to be the thermal average of the quantity

$$\psi(r) = \langle \exp(i6\theta(r)) \rangle \qquad \textbf{2.20}$$

where, the bond angle $\theta(\mathbf{r})$ is the orientation, relative to any fixed laboratory axis, of a bond between two nearest neighbour molecules. The x-ray diffraction patterns have been analysed to determine the temperature dependence of the Bond Orientational Order (BOO) in the smectic B phase. The BOO has been calculated by evaluating the expression,

$$\langle \cos(6\theta) \rangle = \int_0^{\pi/6} \cos(6\theta) f(\theta) d\theta \,/\, \int_0^{\pi/6} \cos f(\theta) d\theta \qquad \textbf{2.21}$$

where, $f(\theta)$ is the angular distribution function of centre of mass of the neighbouring molecules with respect to a central molecule and the angular distribution function has a maximum at $\theta = 0$. The above equation can be approximated by the following expression,

$$\langle \cos(6\theta) \rangle \approx \int_0^{\pi/6} \cos(6\theta) I(\theta) d\theta \,/\, \int_0^{\pi/6} I(\theta) d\theta \qquad \textbf{2.22}$$

where $I(\theta)$ is the azimuthal distribution of the x-ray diffraction intensity. According to Vainshtein [14] it has been assumed that $I(\theta)$, the intensity distribution, is proportional to $f(\theta)$ the distribution function and has its maximum at $\theta = 0$. BOO is calculated for each peak and finally the average over six peaks are taken. The intensity values plotted against azimuthal angular positions have been corrected for the background (scattered) intensity values.

a) Intermolecular distance:

The average lateral distance between the neighbouring molecules (D) is related to the corresponding Bragg angle (2θ) according to the formula [17];

$$2D \sin \theta = k\lambda \qquad \textbf{2.23}$$

where, θ is the Bragg angle for the equatorial diffraction, λ is the wavelength of CuK_α line and k is a constant varying with order parameter [23]. For perfectly ordered state k = 1.117 as given by de Vries [17].

b) Apparent molecular length or layer thickness:

Linear scanning of inner hallo or spot of x-ray diffraction photograph gives the apparent molecular length for nematic phase or layer thickness (d) for smectic phase, by using Bragg equation (2d sinθ =λ).

c) Transverse Correlation Length:

The transverse correlation length is determined from a linear scan of the x-ray diffraction peaks. X-ray intensities are at first corrected for the use of a flat plate camera following inverse square law. This corrected intensity data are then deconvoluted for finite width of the collimator. The deconvoluted intensity profile I(q) is fitted to a Lorentzian form with a quadratic background viz.,

$$I(q) = \frac{a_1}{a_2 + (q - q_o)^2} + a_3 q^2 + a_4 q + a_5 \qquad \textbf{2.24}$$

q being the magnitude of the scattering vector. The transverse correlation length is defined as $\xi = 2\pi(a_2)^{-1/2}$. For this instrument, the in-plane transverse resolution $\Delta q = 6 \times 10^{-3}$ Å^{-1}.

2.8 Refractive index of mesophases:

Most of the nematic liquid crystals are optically uniaxial and strongly birefringent. A uniaxial liquid crystal has two principal refractive indices viz. ordinary refractive index (n_o) and extraordinary refractive index (n_e). The birefringence is defined by the following equation:

$$\Delta n = n_e - n_o \qquad \textbf{2.25}$$

Birefringence of liquid crystals was first determined experimentally by E. Dorn [24] for nematogen. Subsequently Δn was measured in smectic phases [25-32]. Birefringence is positive for conventional nematics with its value lying between 0 to 0.4, while it is negative for chiral nematics. The Δn is related to the molecular polarizability (α), which originates due to π-electrons and delocalised electrons not participating in chemical bonds of the organic sample. As internal field is anisotropic in nature for mesogens, Lorentz-Lorentz force, valid for liquid state, is not applicable here; and the molecular polarizability can be determined by knowing the value of internal field. Saupe and Maier [33] applied a more elaborate internal field suggested by Neugebauer. I have followed the Neugebauer [34] and Vuks [35] modified formula for calculation of α.

i) Neugebauer's Method:

Neugebauer [34] extended Lorentz-Lorentz equations for an isotropic system to an anisotropic system. In this model the effective polarizabilities α_o and α_e of the liquid crystals are related to the refractive indices n_e and n_o according to the following equations:

$$n_e^2 - 1 = \frac{1}{4\pi N\alpha_e(1 - N\alpha_e\gamma_e)} \qquad \textbf{2.26}$$

and

$$n_o^2 - 1 = \frac{1}{4\pi N\alpha_o(1 - N\alpha_o\gamma_o)} \qquad \textbf{2.27}$$

where, γ_o and γ_e are the respective internal field constants for ordinary and extraordinary rays, N is the number of molecules per cm^3 and n_e and n_o are the extraordinary and ordinary refractive indices respectively. The relevant equations for calculating polarizabilities (α_o,α_e) as obtained from the equations 2.26 and 2.27 are as follows

$$\frac{1}{\alpha_e} + \frac{2}{\alpha_o} = \frac{4\pi N}{3}\left[\frac{n_e^2 + 2}{n_o^2 - 1} + \frac{2(n_o^2 + 2)}{n_o^2 - 1}\right] \qquad \textbf{2.28}$$

and

$$\alpha_e + 2\alpha_o = \frac{9}{4\pi N}\left[\frac{n^2 - 1}{n^2 + 2}\right] \qquad \textbf{2.29}$$

where, n is the mean refractive index

$$n^2 = \frac{1}{3}\left(2n_o^2 + n_e^2\right)$$

α_o and α_e values are obtained by directly solving equations 2.28 and 2.29.

ii) Vuks method:

Vuks [35] considered that the internal field is independent of molecular interaction and the corresponding relations are:

$$\frac{n_o^2 - 1}{n_e^2 + 2} = \frac{4\pi N}{3}\alpha_o \qquad \textbf{2.30}$$

and $$\frac{n_o^2 - 1}{n_e^2 + 2} = \frac{4\pi N}{3}\alpha_e \qquad \textbf{2.31}$$

where, $n^2 = \frac{1}{3}\left(2n_o^2 + n_e^2\right)$, n is the mean refractive index.

α_o and α_e can be calculated directly from the refractive index values.

2.9 Calculation of orientational order parameter from the refractive index measurement:

The relation between orientational order parameter $<P_2>$ and the principal polarizabilities are given by de Gennes [36] as

$$\alpha_e = \bar{\alpha} + \frac{2}{3}\alpha_a \langle P_2 \rangle \qquad \textbf{2.32}$$

$$\alpha_o = \bar{\alpha} + \frac{2}{3}\alpha_a \langle P_2 \rangle \qquad \textbf{2.33}$$

where, $\bar{\alpha} = \frac{(2\alpha_o + \alpha_e)}{3}$, is the mean polarizability

and $\bar{\alpha_a} = (\alpha_{\parallel} - \alpha_{\perp})$, molecular polarizability anisotropy

where $\alpha_{\parallel}$ and $\alpha_{\perp}$ are the principal polarizabilities, parallel and perpendicular to the long axes of the molecules in the crystalline state.

From equation 2.32 and 2.33, we obtained

$$< P_2 >= \frac{\alpha_e - \alpha_o}{\alpha_{\parallel} - \alpha_{\perp}} \qquad \textbf{2.34}$$

Due to strong absorption in the crystalline state, we used Haller's extrapolation method [37] to calculate α_a. The graph was plotted with $\log(\alpha_e-\alpha_o)$ vs. $\log(T_c - T)$ giving a straight line which is extrapolated to $\log(T_c)$, where T_c corresponds to nematic isotropic transition temperature. At T = 0 K, i.e., in the crystalline state, $<P_2>$ is considered to be equal to 1and then $(\alpha_\parallel-\alpha_\perp)$ is equal to $(\alpha_e-\alpha_o)$. For a given sample, α_e and α_o are calculated at various constant temperatures from which $(\alpha_\parallel-\alpha_\perp)$ is obtained. The order parameter $<P_2>$ is then calculated by using equation 2.34.

2.10 Measurement of refractive indices:

The principal refractive indices (n_o, n_e) of a liquid crystal were measured using thin hallow prisms with the refracting angle less than 2°. The details of the preparation of the prism and the experimental procedure have already been reported by Zemindar et al [38]. To prepare prism optically flat glass plates are taken, and they are first cleaned with conc. HNO_3.Then washed it with water several times till there is no acid reagent. The glass plates are then dried and then by dipped in acetone to remove any organic impurities. One surface of the glass plates was rubbed on bond paper in a direction parallel to one of their edges. The rubbed surface is then coated with thin layer of 1% solution of polyvinyl alcohol (PVA) and then dried. The preferred direction on the substrate can be obtained by rubbing the same surface in the same direction again by a tissue paper. The prism was then prepared by placing the rubbed surfaces inside, with the rubbing direction parallel to the refracting edge of the prism. A thin glass spacer was introduced between one of the vertical edge of the prism for getting the desired refracting angle of the prism. The glass plates of the prism were

sealed together by using high temperature adhesive and were baked in an oven. Liquid crystal sample was introduced into the prism from its top open side by melting. The system was alternately heated to isotropic phase and cooled slowly so that the liquid crystals were perfectly aligned with its optic axis parallel to the refraction edge of the prism. The prism was then placed inside a brass oven provided with transparent opening at the centre and the temperature of the oven was maintained at a desired value by a temperature controller (Indotherm model IT401D2) within an accuracy of ±0.5 °C. The refractive indices (n_o, n_e) were measured for wavelengths λ = 5890Å, corresponding to mercury source by means of a precision spectrometer and an optical monochromator.

2.11 Measurements of densities:

Measurements of density of the mesogens were performed with the help of a dilatometer of the capillary type. Dilatometer with weighed amount of the liquid crystal was kept immersed in a thermo-stated liquid bath. With the help of travelling microscope the height of the liquid crystal column was measured at different temperatures. Sufficient time was given to attain equilibrium at any desired temperature. The accuracy of density measurement lies within ± 0.1%.

2.12 Magnetic susceptibility measurements:

The orientational order parameter of liquid crystal is related to the magnetic susceptibility [37-39] in a more or less straightforward way. It is widely accepted to be one of the best methods for studying the variation of order parameter with temperature. The determination of diamagnetic properties is

of great importance in the study of liquid crystals. The theoretical treatment regarding the effect of external magnetic field on liquid crystal was given by J. P. Dias [40] and J. O. Kessler [41]. The magnetisation **M** induced by the applied magnetic field **H** is given by,

$$\mathbf{M}_o = \chi_{\alpha\beta}\mathbf{H}_\beta \qquad \alpha,\beta = x,y,z \qquad \textbf{2.35}$$

where $\chi_{\alpha\beta}$ is an element of the magnetic susceptibility tensor $\bar{\chi}$ and the summation convention over repeated index is followed. For uniaxial phase like nematic or smectic A phase and choosing the director **n** along the z-axis we have

$$\bar{\chi} = \begin{bmatrix} \chi_\perp & 0 & 0 \\ 0 & \chi_\perp & 0 \\ 0 & 0 & \chi_\parallel \end{bmatrix}$$

The subscript $\chi_\parallel$ and $\chi_\perp$ are the components parallel and perpendicular to the director respectively. The average susceptibility is given by

$$\bar{\chi} = \frac{1}{3}\sum_r \chi_{rr} = \frac{1}{3}(\chi_\parallel - 2\chi_\perp) \qquad \textbf{2.36}$$

The magnetic susceptibility anisotropy is defined as

$$\Delta\chi = (\chi_\parallel - \chi_\perp) = \frac{3}{2}(\chi_\parallel - \bar{\chi}) \qquad \textbf{2.37}$$

Hence the susceptibility tensor has only two different non zero elements,

$\mathbf{M} = \chi_\parallel \mathbf{H}$, if **H** is parallel to **n**

$\mathbf{M} = \chi_\perp \mathbf{H}$, if **H** is perpendicular to **n**

For an arbitrary angle (θ) between **H** and **n** we derive for total magnetisation

$$\mathbf{M} = \chi_\perp \mathbf{H} + \Delta\chi(\mathbf{H}.\mathbf{n})\mathbf{n} \qquad \textbf{2.38}$$

Therefore the free energy in a magnetic field is given by:

$$\mathbf{F}_m = -\int_0^H \mathbf{M}\cdot d\mathbf{H}$$

$$= \frac{1}{2}\chi_\perp \mathbf{H}^2 - \frac{1}{2}\Delta\chi(\mathbf{H}\cdot\mathbf{n})^2 \qquad \textbf{2.39}$$

Since the first term of the above equation is free from **n**, it may be omitted as far as orientation related problems are concerned. For positive anisotropy i.e. $\Delta\chi > 0$, the last term is minimised when **H** is collinear with **n**. Therefore the liquid crystal with positive $\Delta\chi$ tend to align with their molecular long axes along the direction of the applied magnetic field. However, for liquid crystal with negative$\Delta\chi$, the molecules tend to align perpendicular to the applied magnetic field.

2.13 Relation between order parameter and magnetic anisotropy:

The order parameter Q is defined by considering the anisotropic part of the susceptibility χ as follows,

$$Q_{\alpha\beta} = \chi_{\alpha\beta} - \delta_{\alpha\beta}\overline{\chi} \qquad \textbf{2.40}$$

where, $\alpha,\beta = x,y,z$ and $\delta_{\alpha\beta}$ is the kronecker delta function, S is a second rank tensor, which is diagonal. Considering the director **n** along the z-axis, then Q has zero trace and vanishes for the isotropic phase. If we consider uniaxial symmetry around **n**, it is sufficient to consider only one element Q_{zz}. Equation 2.40 can also be written as

$$Q_{\alpha\beta} = \chi_{\alpha\beta} - \frac{1}{3}\delta_{\alpha\beta}\sum_\gamma \overline{\chi}_{\gamma\gamma} \qquad \textbf{2.41}$$

$$\text{then,}\quad Q_{ZZ} = \chi_{ZZ} - \frac{1}{3}(\chi_{XX} + \chi_{YY} + \chi_{ZZ})$$

$$\text{Therefore,}\quad Q_{ZZ} = \frac{2}{3}(\chi_\parallel - \chi_\perp) \qquad \textbf{2.42}$$

Here we have assumed, $\chi_{XX} = \chi_{YY} = \chi_\perp$ **and** $\chi_{ZZ} = \chi_\parallel$

In order to relate Q to the microscopic order parameter S, let K be the tensor of the molecular magnetic polarizability which is assumed to be diagonal in the molecule - fixed co-ordinate system ξ,η,ζ.

Therefore, $$\chi_{\alpha\beta} = N\sum_{i,j} K_{ij} < i_\alpha \; j_\beta > \qquad 2.43$$

where $i, j = \xi,\eta,\zeta$; $\alpha, \beta =$ x, y, z and i_α is the α - component of a unit vector along ξ,η,ζ axes, N is the number of molecules per unit volume and the bracket $< >$ stands for statistical average.

The order parameter represented by equation 2.41 can be expressed in terms of equation 2.43, as $$Q_{\alpha\beta} = N\sum_{i,j} K_{ij} < i_\alpha \; j_\beta - \frac{1}{3}\delta_{\alpha\beta}\delta_{ij} > \qquad 2.44$$

Therefore,
$$Q_{ZZ} = N\sum_{i,j} K_{ij} < i_Z \; j_Z - \frac{1}{3}\delta_{ij} >$$
$$= \frac{2}{3}N\sum_{i,j} K_{ij}\frac{1}{2} < 3i_Z \; j_Z - \frac{1}{3}\delta_{ij} >$$
$$= \frac{2}{3}N\sum_{i,j} K_{ij}S_{ij} \qquad 2.45$$

where, $S_{ij} = \frac{1}{2} < 3i_Z \; j_Z - \delta_{ij} >$ is the generalised order parameter. Thus from equation 2.42 and 2.45 we have,

$$Q_{ZZ} = \frac{2}{3}(\chi_{\parallel} - \chi_{\perp})$$
$$= \frac{2}{3}N\sum_{i,j} K_{ij}S_{ij} \qquad 2.46$$

As S_{ij} is diagonal in a molecular fixed coordinate system ξ, η, ζ with the ζ-axis as the long molecular axis and has zero trace, there are two independent scalar order parameter, for which we choose $S = S_{\zeta\zeta}$ and $D = S_{\eta\eta} - S_{\zeta\zeta}$.

Thus equation 2.46 can be written as

$$\frac{(\chi_{\parallel} - \chi_{\perp})}{N} = \{K_{\xi\xi} - \frac{1}{2}(K_{\eta\eta} + K_{\xi\xi})\}S + \frac{1}{2}(K_{\xi\xi} - K_{\eta\eta})D \qquad 2.47$$

where S is the order parameter which have a value between 0 and 1.

Thus, $$<S>=\frac{1}{2}<3\xi_z^2-1>$$

Therefore, $$<S>=\frac{1}{2}<3\cos^2\theta-1>$$

where 'θ' is the angle between z and ζ axes.

Furthermore, $$D=\frac{1}{2}<3\xi_z^2-1>-\frac{1}{2}<3\eta_z^2-1>$$

$$=\frac{3}{2}<\xi_z^2-\eta_z^2>$$

$$=\frac{3}{2}<\sin^2\theta\cos2\psi>$$

where ψ is the Euler angle specifying the rotation around the ζ-axis. D measures the difference in tendency of the two transverse molecular axes to project on the z-axis. By considering the molecule to be axially symmetric, we have D = 0.

Now equation 2.47 can be written as,

$$<S>=\frac{(\chi_{\parallel}-\chi_{\perp})}{(\chi_l-\chi_t)} \qquad \textbf{2.48}$$

where $\chi_l = NK_{\xi\xi}$ and $\chi_t = \frac{1}{2}N(K_{\eta\eta}+K_{\xi\xi})$

Equation 2.47 is known as Tsvetkov's expression for order parameters [42]. To determine the order parameter (S) we need the value of (χ_l - χ_t) which can be obtained from solid single crystal measurements. In the present case (χ_l - χ_t) is determined by Haller method [37]. (χ_l - χ_t) plotted against ln(T_c-T) extrapolated to a point T = 0°K where S is assumed to be unity.

2.14 Determination of χ:

The magnetic susceptibility has been measured by the classical Faraday-Curie method. The total force (F) experienced by a sample in an

inhomogeneous magnetic field with a gradient in the horizontal x-direction is given by

$$F = \frac{1}{2}(m\chi - m_0\chi_0)\left(\frac{dH^2}{dx}\right)_{avg} \qquad 2.49$$

where χ, m are the mass susceptibility and the mass of the sample and χ_0, m_0 are those of air driven out of the sample. The subscript 'avg' indicates the average value. If we assume that the sample is replaced by almost same volume of the reference sample and is placed at more or less at the same position between the pole pieces of the magnet, then (dH^2/dx) will be same for both the cases. By indicating the reference sample with the subscript 'r', the force acting on the reference sample is given by:

$$F = \frac{1}{2}(m_r\chi_r - m_0\chi_0)\left(\frac{dH^2}{dx}\right)_{avg} \qquad 2.50$$

Using equation 2.49 and 2.50 the magnetic susceptibility can be written as

$$\chi(t) = \frac{Fm_r}{F_r m}[\chi_r - \frac{\rho_0(t_0)}{\rho_r(t_0)}\chi_0(t_0)] + \frac{\rho_0(t)}{\rho(t)}\chi_0(t) \qquad 2.51$$

where ρ, ρ_r and ρ_0 are densities of the experimental sample, reference sample and air respectively; t_0 is the temperature at which the measurement of the reference sample is made.

The sample was put in a cylindrical quartz container having a volume of nearly 0.1 cm^3. It was hung by a glass capillary between the pole pieces, the value of (dH^2/dx) being 1.1 K. $gauss^2$ / cm approximately. The variation of (dH^2/dx) is 1% over a distance of 1cm along x-direction, while along y and z direction it is practically constant over sufficiently large distances. The temperature of the sample was controlled by temperature controller (Indotherm model 401 D2) having accuracy $\pm 0.5^{\circ}C$. The whole system is

evacuated to avoid disturbance to the balance due to convection in air. The accuracy of measurement using this balance is about 1%.

Trans-decaline a non-volatile liquid at room temperature having $\chi_r = 0.779 \times 10^{-6}$ cm^3 gm^{-1} [43] and density ρ_r=0.869 gm cm^{-3} [44] was used as a reference substance. The necessary correction term in equation 2.51 for $\chi_o(t)$ can be calculated by using the tabulated density of air [45], the magnetic susceptibility of air ($\chi_o = 106.3 \times 10^{-6}$ cm^3 gm^{-1} at 20°C) [46] and the use of curie law $\chi_o \sim 1/T$. I have also neglected the influence of dissolved oxygen as discussed and ignored by de Jeu et al [47].

In the experimental arrangement, the force acting on the sample is exactly balanced by the force exerted on the horizontal coil rigidly attached to the beam balance, placed inside a hollow permanent magnet with a uniform radial field and carrying a suitable current i.

$$F = 2\pi rniH \qquad \textbf{2.52}$$

where, n is number of turns in the coil, r is the radius of the coil and H is the magnetic field intensity. In general the suspended system will experience a force even in the absence of any sample due to the diamagnetism of the sample holder. To compensate this pull an initial current i_o is passed through the coil. In this case, the potential drop across a standard resistance of the order 10KΩ with the help of precision digital voltmeter has been measured. So the final expression for the susceptibility becomes,

$$\chi(t) = \frac{(V - V_o)m_r}{(V_r - V_o)m}\left[\chi_r - \frac{\rho_o(t_o)}{\rho_r(t_o)}\chi_o(t_o)\right] + \frac{\rho_o(t)}{\rho(t)}\chi_o(t) \qquad \textbf{2.53}$$

All the values of magnetic susceptibilities given by me in this thesis are mass susceptibility in c.g.s. unit (erg $gauss^{-2}$ gm^{-1}).

2.15 Description of the experimental set-up for determination of diamagnetic susceptibilities:

The electromagnetic balance for measuring susceptibilities have been designed and fabricated in our laboratory by M. Mitra and R. Paul [48]. Basically the instrument is of the Curie type, the movement of the arms being restricted to the horizontal plane. Schematic diagram of which is shown in Figure 2.3. A horizontal light glass beam (A) is kept suspended at the middle with vertically stretched phosphor-bronze strips (S). The upper portion of which is soldered to a torsion head T, used for adjusting the position of the beam, whereas, the lower end of it terminates in an elliptic spring (E) secured to a universal adjustable holder (H) which can be moved horizontally in two directions. The torsion head is fixed to a brass pillar (D), which serves the electrical connectivity with the brass plate (B) as well. The holder (H) is also fixed on a flat brass plate (B) resting on levelling screws (W). A small perspex block (R) is fixed at one end of the beam balance which is attached to a long glass capillary tube (U) carrying a small glass capsule type sample holder (L) passing through a vertical hole (h2). A damping vane (V) made of thin mica sheet dipping into diffuse pump oil fixed to the other side of the glass beam effectively damps out all spurious vibrations. On the same side of the balance beam is attached a balancing coil of 50 turns of 42 s.w.g. enamelled copper wire wound over a hollow perspex cylinder (C) and the coil is free to move inside a hollow magnet (M) having a radial field of about 200 gauss. The balance assembly is covered with a greased ground bell jar (J). Two holes h1 and h2 are drilled in the base plate. In one of this hole, is fixed an ebonite block with binding terminal, sealed vacuum tight with araldite, for leading in the coil currents. The other terminal of the coil is attached to the brass plate. The second aperture (h2) is

about 3 cm in diameter is fitted with a brass collar for fitting the glass tube extension of the experimental chamber.

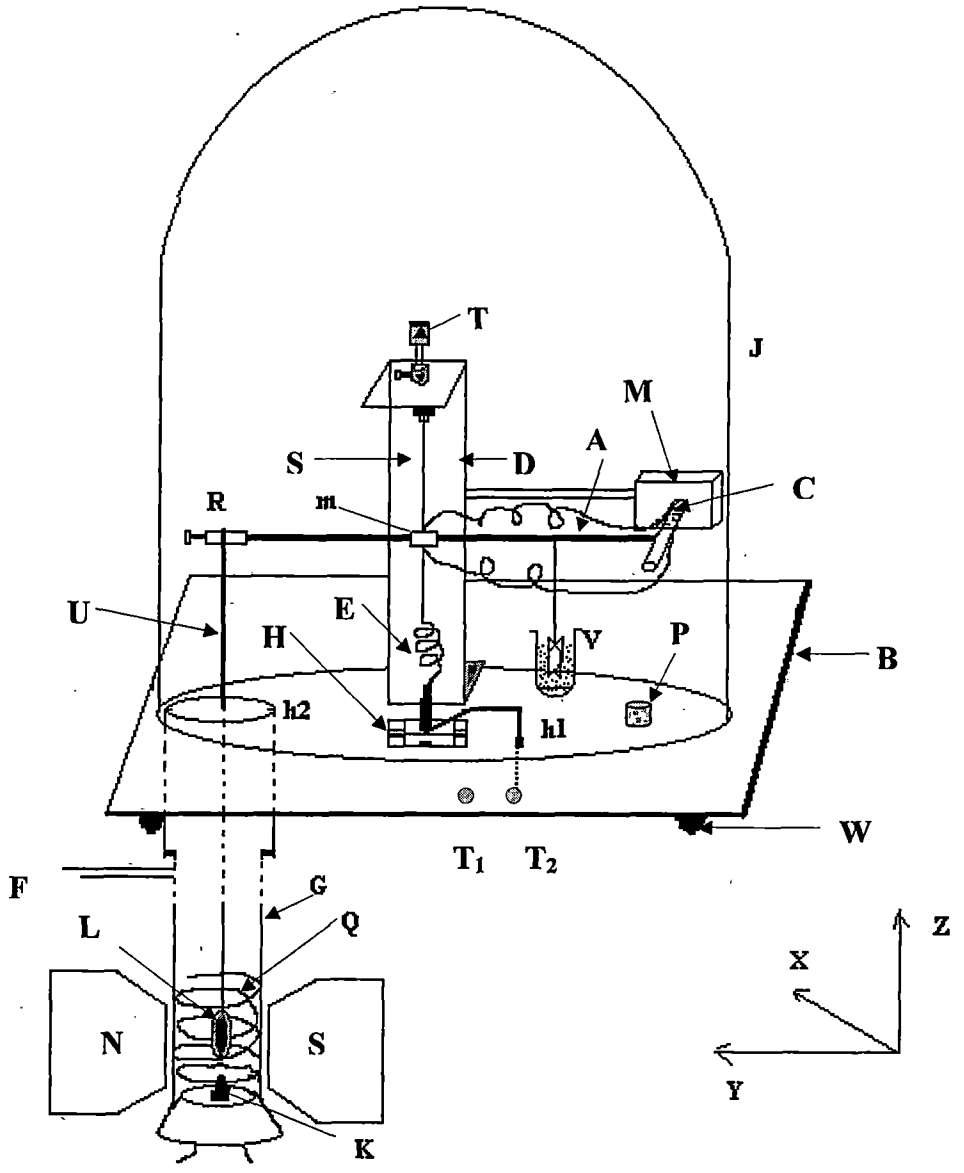

FIGURE 2.3: Schematic diagrams of magnetic susceptibility apparatus.
T- Torsion head, **D**- Brass pillar, **S**- Phosphor-bronze strip, **m**- mirror, **A**- Balance beam, **M**- Magnet, **C**- Coil, **E**- Spring, **G**- Glass tube, **Q**- Heater, **K**- Thermo-couple, **P**- Beaker Containing calcium chloride, **V**- Damping vane, **H**- Adjustable platform, **J**- Bell jar, **B**- Brass plate, **R**- Perspex block, **h1**and **h2**- holes through the brass plate, **U**- Glass capillary tube, **L**- Sample holder, **F**-Side tube connected to vacuum pump, **W**- Levelling screw, T_1-Terminal connected with brass plate & T_2 that with the spring.

The joint of the glass tube (G) and brass tube is made vacuum tight with o-ring. A heater (Q) of constantant wire and a thermocouple (K) is fixed through a rubber stopper and is introduced into the glass tube, which is made vacuum tight. The sample holder, thermocouple and the heater are placed between the pole pieces of an electromagnet. The brass tube is also provided with a side tube (F) through which the balance chamber and the experimental chamber can be evacuated. The sucksmith form of a pole piece is adopted and any change in the position of the sample was detected with the help of a photocells. A laser beam of low intensity is focused on the mirror (m) fixed at the centre of the glass balance and the reflected beam is detected by the photocells, the electrical signal is then amplified and feed to a sensitive moving coil galvanometer, for detecting any change in the position of the sample holder. It should be notated that since the director of the mesogens aligns itself in the direction of the magnetic field ($\Delta\chi > 0$) in most samples, the magnetic susceptibility determined by this method is $\chi_{\parallel}$ in mesophase and $\bar{\chi}$ in isotropic phase. Since non-metallic organic mesogens are diamagnetic, $\bar{\chi}$ should be independent of temperature. Therefore, magnetic susceptibility anisptropy $\Delta\chi$ is calculated by using equation 2.37. Thus the order parameter $\langle S \rangle$ is then calculated using equation 2.48.

2.16 Dielectric permittivity measurement:

One can study the response of the mesogenic substances to the application of electric field by its dielectric behaviour. The liquid crystal molecules may possess permanent dipole moments; in addition induced dipoles are created when external field is applied. Due to the geometrical anisotropy in the molecular structures liquid crystals exhibits anisotropic behaviour. One can

determine $\varepsilon_{\parallel}$ and $\varepsilon_{\perp}$, parallel and perpendicular components of dielectric permittivity by applying electric field parallel and perpendicular to the director. A brief description of experimental set-up is shown in figure 2.4. The dielectric permittivity was measured by a digital LCR-bridge at 10 KHz. The liquid crystal samples were filled in a glass cell. The construction of the cell was done by means of two plane parallel indium tin oxide (ITO) coated (thickness 7000Å and conductivity 10.5-11.5 Ω/square) glass plates separated by glass-spacer of thickness 120μm. The cell was equipped with a guard ring to avoid errors due to stray fields. The guard ring was produced by etching the conducting surfaces on the glass plates. The effective electrode area was 2.3cm x 1.5cm.

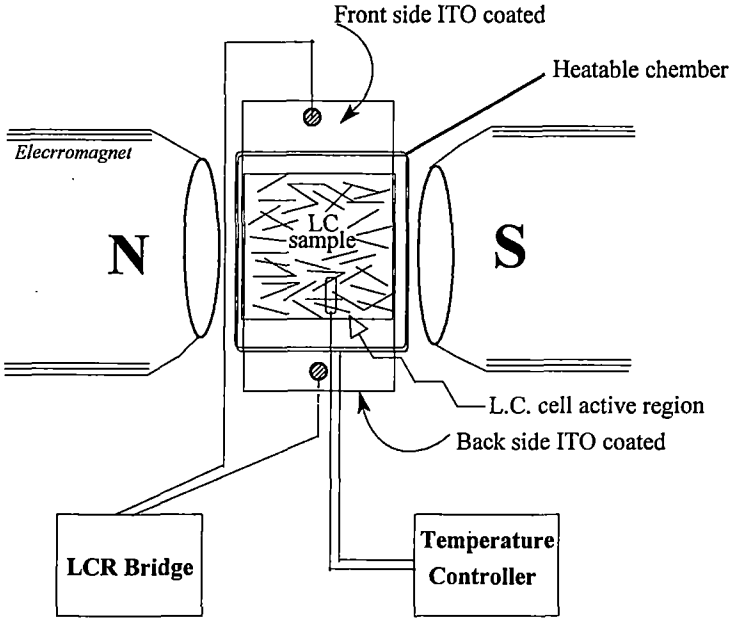

FIGURE 2.4: Schematic diagram of experimental setup for dielectric constant measurement.

The cell was kept inside an electrically heated thermostated brass block having dimension 2.6cm x 2.8cm x 0.5cm, whose temperature was accurately controlled within ±0.5°C using a temperature controller

(Indotherm-457). The whole system was placed between the pole pieces (area 40cm^2, pole gap 3.5cm) of an electromagnet whose field strength could be varied up to 0.32T. The cell was calibrated by measuring the capacitances of standard dielectric liquids within an accuracy of 1%. To determine $\varepsilon_{\parallel}$ and $\varepsilon_{\perp}$, the parallel and perpendicular components of dielectric permittivity capacitances C_a, C_b and C_x of the cell filled with air, benzene (as standard materials) and the liquid crystal sample respectively were measured by applying electric field parallel and perpendicular to the director of the liquid crystal using the following expression

$$\varepsilon_x = 1 + \frac{(C_x - C_a)}{(C_b - C_a)}(\varepsilon_b - 1) \qquad \textbf{2.54}$$

where ε_b and ε_x are the relative permittivities of benzene and the liquid crystalline substance; and that of air is taken as unity.

The dielectric constants $\varepsilon_{\parallel}$ and $\varepsilon_{\perp}$ were determined by measuring the capacitance of the cell with and without the sample at various temperatures keeping the magnetic field parallel and perpendicular to the director respectively [49-52]. The capacitance of the empty cell was found to be 27.4pF at 20°C. Alignment of the sample was established by observing the saturation value of capacitance as magnetic field was increased to about 0.3T. It may be mentioned here that in a magnetic field of about 0.3T we have been able to take well aligned x-ray diffraction photographs in both nematic as well as smectic phases. Since the liquid crystal samples studied are highly insulating the contributions to the capacitance from space charges could be neglected.

2.17 Elastic constant and deformation free energy of nematic liquid crystal:

The elastic properties of a liquid crystal are generated due to restoring torques, which become apparent when the system is perturbed from its equilibrium configuration by some external electric or magnetic field. The director pattern is no longer uniform in space, but curved. If n(r) changes noticeably only over a large distances compared to the molecular dimensions, this curvature can be described in terms of a continuum theory which disregards the details of the structure on a molecular scale. Based on this viewpoint, Zocher [53], Oseen [54], and Frank [55] developed a phenomenological continuum theory of liquid crystals that can successfully explain the various magnetic or electric field induced effect of liquid crystals. According to the continuum theory of liquid crystals, the elastic part of the internal energy density of a perturbed liquid crystal is given by the equation,

$$\mathbf{F}_{def} = \frac{1}{2}[\mathbf{K}_{11}(\nabla \cdot \mathbf{n})^2 + \mathbf{K}_{22}(\mathbf{n} \cdot \nabla \times \mathbf{n})^2 + \mathbf{K}_{33}(\mathbf{n} \times \nabla \times \mathbf{n})^2] \qquad \mathbf{2.55}$$

where **n** is the director; and the coefficients K_{11}, K_{22}, K_{33} are so-called elastic constants associated with three basic types of distortions viz., splay, twist, and bend respectively and are collectively known as the Frank elastic constants. The above equation is the fundamental formula for the continuum theory of nematics. It is possible to generate deformations that are pure splay, pure twist or pure bend. Thus each constant should be positive, if not, the undistorted nematic conformation would not corresponds to a minimum of the free energy F_{def}.

2.18 Fréedericksz transition:

The elastic constants of the liquid crystals can be determined by various methods, of which Fréedericksz transition is one of the simplest and convenient methods. The term Freedericksz transition refers to the deformation of a thin layer of nematic liquid crystal sample with a uniform director pattern in an external electric [56-59] or magnetic field [60-67]. Fréedericksz observed that when a planar surface aligned nematic liquid crystal cell is subjected to magnetic field normal to the director then the cell undergoes an abrupt change in its optical properties if the strength of the external field exceeds the threshold value, known as the critical field. If the nematic liquid crystals have positive diamagnetic anisotropy or dielectric anisotropy, then as the field exceeds the critical value, the director starts to align along the external field. Fréedericksz transitions can be use to measure directly the elastic constants, provided the geometry i.e., the boundary conditions and the direction of the applied field are chosen in a appropriate way as shown schematically in figures 2.4.

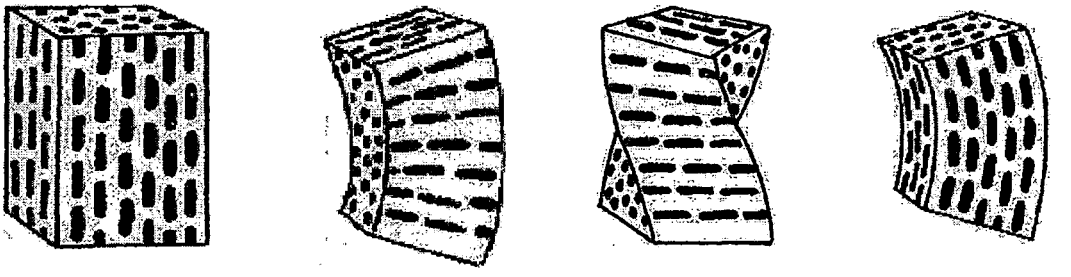

Equilibrium Configuration **Splay** **Twist** **Bend**
(a) (b) (c) (d)

FIGURE 2.4: (a) An ordered liquid crystal in equilibrium configuration. The deformation states – (b) splay, (c) twist, and (d) bend.

From the geometry of arrangement as shown in figure 2.5(a-c), one can determine the splay, twist or bend elastic constants in the magnetic field H.

The threshold magnetic field for the splay, bend or twist deformation is related to the elastic constants by the equation

$$(H_C)_i = \frac{1}{2}\left(\frac{K_{ii}}{\Delta\chi}\right)^{\frac{1}{2}}\frac{\pi}{d} \qquad 2.56$$

where d is the sample thickness, $\Delta\chi$ is the diamagnetic anisotropy and $(H_c)_i$ is the respective critical magnetic field. Also the subscript i =1, 2, 3 refers to the splay, twist and the bend deformation respectively.

To explain the Fréedericksz transition, I have considered a uniform planer layer i.e., in the splay mode, for a magnetic field $H>H_c$, applied along z-axis, the uniform planer structure (figure 2.5(d)) is unstable and the system jumps into one of the two possible states (figure 2.5(e) or 2.5(g)). If the field is increase further ($H >> H_c$) these states develop into pattern as shown in figure 2.5(f) and 2.5(h).

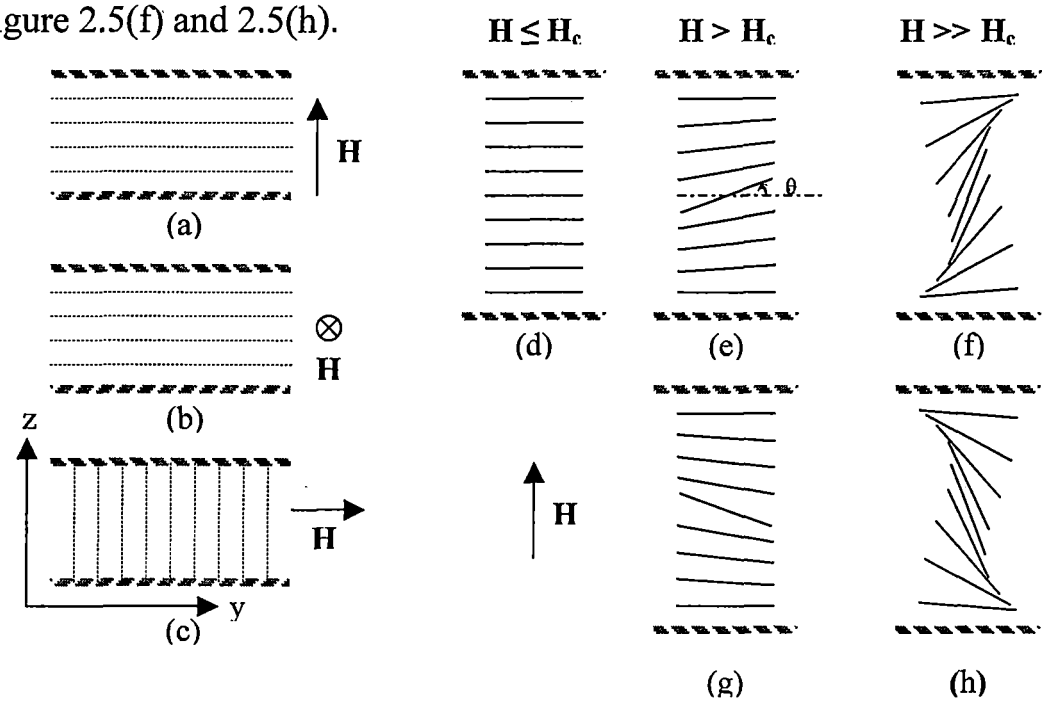

FIGURE 2.5: Schematic experimental set-up for determination of (a) splay, (b) twist, and (c) bend; Deformation of director pattern above threshold field in the splay (d-h) mode.

2.19 Description of Experimental set-up for determination of K_{11} and K_{33}:

The apparatus of the determination of the elastic constants (K_{11} and K_{33}) has been designed and fabricated in our laboratory by M. K. Das and R. Paul [68]. The block diagram of the experimental set-up has been shown in figure 2.6 for studying elastic constants by Freedericksz transition method.

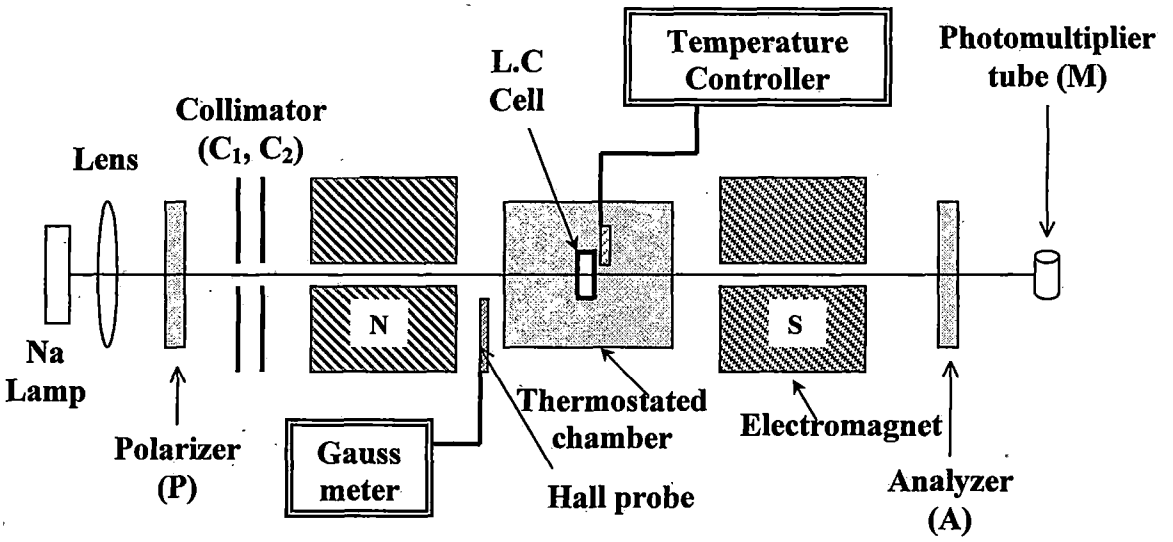

FIGURE 2.6: Schematic experimental set-up for the determination of the elastic constants from Freedericksz transition: (a) splay, (b) twist and (c) bend.

The liquid crystal sample was taken in a glass cell housed in a thermo-stated brass oven that has a groove at the proper angle, whose temperature was controlled within an accuracy of ± 0.5°C by means of a temperature controller (Indotherm model 457). A monochromatic beam of sodium-D light is incident on the sample through a lens (L), polarizer (P) and collimating circular slits (C_1, C_2). The transmitted light intensity was detected by a photomultiplier tube (M) that counts photon and corresponding current was measured by a nano-ammeter. The polarizer (P) and the analyzer

(A) were placed in crossed position (at ±45° relative to the vertical axis) in front of the photomultiplier. For the Fréedericksz transition to occur, the director must be truly oriented at right angle to the external field. In order to ensure this exact alignment, the brass oven was mounted on a specially constructed platform whose alignment with respect to the field could be adjusted to an accuracy of 1-2′ of arc. The magnetic field is varied slowly so that the nematic orientation remains in equilibrium with the applied magnetic field. For desired temperature, it was observed that when the field (H) exceeds a critical value (H_c) then there was a drastic change in the optical properties of the sample. Thus we could measure the threshold field intensity (H_c) from the field versus intensity curve within an accuracy of ±10 Gauss. The magnetic field was measured using a Hall-probe Gaussmeter (Model DGM-102). If the field was increased gradually beyond its critical value, the transmitted light exhibits oscillations due to the change of phase relation.

The liquid crystal sample is taken between two plane parallel glass plates separated by glass spacer of thickness 160μm. The splay elastic constant (K_{11}) is measured using a cells with homogeneous planer alignment, where inside surface of the glass plates were treated with 1% aqueous solution of polyvinyl alcohol dried and then rubbed the layer in one direction with tissue paper. Whereas in case of bend elastic constant (K_{33}) measured by using homeotropic cells, which were prepared by the surface treatment of the glass plates with dilute solution of cetyl tri-methyl ammonium bromide (CTAB) or lecithin.

In the present set-up it is not possible to measure K_{22}. The threshold field for twist deformation cannot be detected optically when viewed along the twist axis. Due to the large birefringence of the medium for this direction of propagation, the state of polarisation of the transmitted beam is indistinguishable from that of the emerging beam from the untwist nematics. A total internal reflection technique can be used to measure the K_{22} values of the twist deformation. In my present work however, I have measured only K_{11} and K_{33} values at different composition of a binary liquid crystalline mixture.

2.20 Structure and chemical name of the liquid crystals studied:

The chemical names of the liquid crystals studied in the present investigation and their structural formula are given below:

1. 4-n-pentyl phenyl 4 - n′- pentyloxy benzoate (ME5O.5 in short).

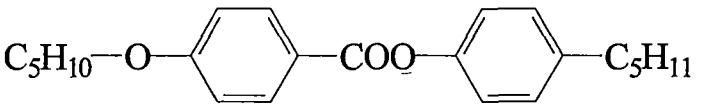

2. 4-n-pentyl 4′ cyanobiphenyl (5CB in short).

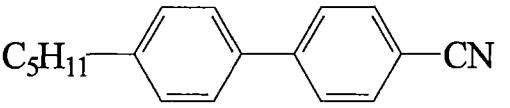

3. undecycloxy cyanobiphenyl (11OCB in short).

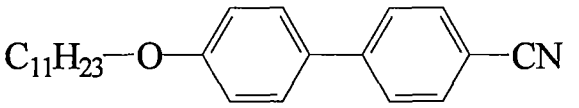

4. 4-n-hexyl phenyl 4-n′-pentyloxy benzoate (ME6.O5 in short).

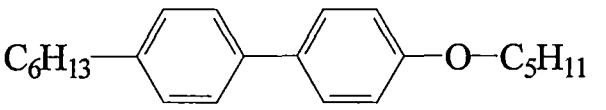

5. 4-n-pentyl phenyl 4-n′-hexyloxy benzoate (ME6O.5 in short).

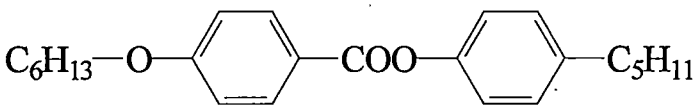

6. p-cyanophenyl trans –4-pentyl cyclohexane carboxylate (CPPCC in short)

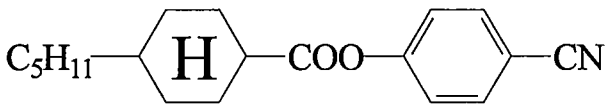

7. 4(3"-pentenyl) 4′(ethoxyl) 1,1′ bicyclohexane (1d(3)CCO_2) in short)

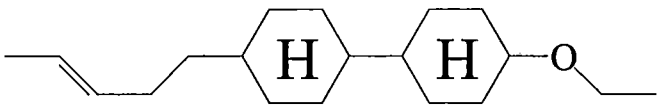

8. 4-ethoxy, 4′-Pent-4"-enyl bicyclohexane (0d(4)CCO_2) in short)

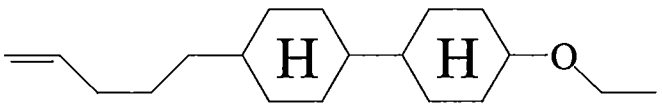

The liquid crystals 1, 2, 3, 4, 5, 6 were obtained from E. Merck, UK; and 7, 8 were obtained from M/S Hoffmann-La Roche & Co., Basel, Switzerland. All the samples were obtained in the pure state and were studied without further purification.

References:

1. E. B. Priestley, P. J. Wojtowicz and P. Sheng, (Eds.), *"Introduction to Liquid Crystals"*, Plenum, New York, (1974).
2. S. Chandrasekhar, *"Liquid Crystals"*, Cambridge University Press, Cambridge, (1977).
3. G. Vertogen and W. H. de Jue, *"Thermotropic Liquid Crystals, Fundamentals"*, Springer-Verlag (1988).
4. G. R. Luckhurst and G. W. Gray, (Eds.), *"The Molecular Physics of Liquid Crystals"*, Academic Press (1979).
5. P. G. de Gennes, *"The Physics of Liquid Crystal"*, Clarendon Press, Oxford, (1974).
6. G. H. Brown, (Ed.), *"Advances in Liquid Crystals"*, **6**, Chapter 1, Academic Press (1983).
7. W. Maier and A. Saupe, *Z. Natureforch*, **13a**, 564 (1958); ibid., **14a**, 882 (1959); ibid., **15a**, 287 (1960).
8. W. L. McMillan, *Phys. Rev.*, **A4**, 1238 (1971).
9. R. L. Humphries, P. G. James and G. R. Luckhurst, *J. Chem. Soc., Faraday Trans. II*, **68**, 1031 (1972).
10. W. L. McMillan, *Phys. Rev.*, **A6**, 936 (1972).
11. K. K. Kobayashi, *J. Phys. Soc.* (Japan), **29**, 101 (1970).
12. K. K. Kobayashi, *Mol. Cryst. Liq. Cryst.*, **13**, 137 (1971).
13. D. Demus and L. Richter, *"Textures of Liquid Crystals"*, Verlag Chemie, New York (1978).
14. B. K. Vainstein and I. G. Chistyakov, *"Problem of Modern Crystallography"*, Nauka, Moscow (1975).

15. B. K. Vainstein, *"Diffraction of x-rays by Chain Molecules"*, Elsevier Pub. Co. (1966).

16. A. J. Leadbetter, *"The Molecular Physics of Liquid Crystals"*, Eds. G. R. Luckhurst & G. W. Gray, Chap.13, Academic Press (1979).

17. A. de Vries, *Mol. Cryst. Liq. Cryst.*, **10**, 219 (1970).

18. B. Jha and R. Paul, *Proc. Nucl. Phys. Solid State Phys. Symp.*, India, **19c**, 491 (1976).

19. H. P. Klug and L. E. Alexander, *"X-ray diffraction procedures"*, John Wiley and Sons, N.Y., p.114 and 473 (1974).

20. A. J. Leadbetter and E. K. Norris, *Mol. Phys.*, **38**, 669 (1979).

21. R. J. Birgeneau and J. D. Litster, *J. Phys. Letts.*, **39**, L399, (1978).

22. A. de Vries, *Liquid Crystals*, Ed. F. D. Saeva, M. Dekker Inc., NY(1979).

23. R. Paul and G. Chaudhuri, Abstract in the 14th International Liquid Crystal Conference, Pisa, 1992, Abs.no.- H-P23.

24. E. Dorn, *Z. Physik*, **11**, 111, (1910).

25. E. Gorecka, Li Chen, O. Lavrentovich and W. Pyzuk, *Europhysics Letters*, **27(7)**, 507 (1994).

26. O. Weiner, S. Ber. Sachs. Ges. Wissensch., **61**, 113 (1909).

27. W. H. Pness, S. A. Teukolsky, W. T. Vellering and B. P. Flannery, Cambridge University Press, Chap- 15. (1986).

28. S. Ergun, *J. Appl. Cryst.*, **1**, 19 (1968).

29. H. Zocher, *Naturwiss.*, **13**, 1015 (1925).

30. H. Zocher, *Z. Krist.*, 79, 122 (1931).

31. F. Grandjean, *Compt. Rend.*, **168**, 408 (1919).

32. N. V. Madhusudana, R. Sashidhar and S. Chandrasekhar, *Mol. Cryst. Liq. Cryst.*, **13**, 61 (1971).

33. A. Saupe and W. Maier, *Z. Natureforsch*, **16a**, 816 (1961).

34. H. E. Neugebauer, *Canad. J. Phys.*, **32**, 1 (1954).

35. M. F. Vuks, *Optics and Spectroscopy*, **20**, 361 (1966).

36. P. G. de Gennes, *Mol. Cryst. Liq. Cryst.*, **12**, 193 (1971).

37. I. Haller, H. A. Huggins, H. R. Lilienthal and T. R. McGuire, *J. Phys. Chem.*, **77**, 950 (1973).

38. A. K. Zeminder, S. Paul and R. Paul, *Mol. Cryst. Liq. Cryst.* , **61**, 191 (1980).

39.P. G. de Gennes, *"The Physics of Liquid Crystal"*, Clarendon Press, Oxford, p.31 (1974). (1961).

40. J. P. Dias, *C. R. Acad. Sci.*, Se'r, **A282**, 71 (1976).

41. J. O. Kessler, *Liq. Cryst. Ord. Fluids*, p. 361 (1970).

42. V. Tsvetkov, *Acta Physicochim.* USSR, **16**, 132, (1942).

43. CRC Handbook of Chemistry and Physics, 58th edition, p. E-128. (1977-78).

44. CRC Handbook of Chemistry and Physics, 58th edition, p. C-270 (1977-78).

45. CRC Handbook of Chemistry and Physics, 58th edition, p. F-9 (1977-78).

46. A. Burris and C. D. Hause, *J. Chem. Phys.*, **11**, 442 (1943).

47. W. H. de Jue and W. A. P. Claassen, *J. Chem. Phys.*, **68**, 102 (1978).

48. M. Mitra and R. Paul, *Mol. Cryst. Liq. Cryst.*, **148**, 185 (1987).

49. A. Christine Rauch, Shila Garg and D.T. Jacobs, *Phase transitions in a nematic binary mixture, J. Chem. Phys*, **116**, 2213(2002).

50. Shila Garg and Tom Spears, Dielectric properties of nematic binary mixture. *Mol. Cryst. Liq. Cryst.*, **409**, 335(2004).

51.H. Kresse, (Ed.) G. H. Brown *Dielectric behaviour of liquid crystal, Adv. Liquid Crystal*, **6**, 109 (1983).

52. W. Haase and S. Wróbel (Eds.), *Relaxation Phenomena*, (2003).

53.H. Zocher, *Trans Faraday Soc.*, **29**, 945 (1933).

54. C. W. Oseen, *Trans Faraday Soc.*, **29**, 883 (1933).

55. F. C. Frank, *Faraday Soc. Discussion*, **25**, 19 (1958).

56. H. Gruler, T. J. Schiffer and G. Meier, *Z. Natureforsh*, **27a**, 966 (1972).

57. H. Gruler and L. Cheung, *J. Appl. Phys.*, **46**, 5097 (1975).

58. H. Deuling, (Ed.) L. Liebert, *Liquid Crystals, Solid State Physics* Suppl. no. 14, p. 77, Academic Press, NY.

59. M. J. Bradshaw and E. P. Rayens, *Mol. Cryst. Liq. Cryst.*, **72**, 35 (1980).

60. V. Freedericksz and V. Tsvetkov, *Phy. Z. Soviet Union*, **6**, 490 (1934).

61. V. Freedericksz and V. zolina, *Trans. Faraday Soc.*, **29**, 919 (1933).

62. P. P. Karat and N. V. Madhusudana, *Mol. Cryst. Liq. Cryst.*, **40**, 239 (1977).

63. H. P. Schad, M. A. Osman, *J. Chem. Phys.*, 75 (2), 880 (1981).

64. F. Leenhouts, H. J. Boeber, A. J. Dekker and J. J. Jonker, *J. Phys. (Paris) Colloque.*, **40**, C3-291 (1979).

65. H. P. Schad, G. Bauer and G. Maier, *J. Chem. Phys.*, **67**, 3705 (1977).

66. F. Leenhouts and A. J. Dekker, *J. Chem. Phys.*, **74**, 1956 (1981).

67. H. P. Schad, G. Bauer and G. Maier, *J. Chem. Phys.*, **70**, 2770 (1979).

68. M. K. Das and R. Paul, *Mol. Cryst. Liq. Cryst.*, **259**, 13 (1995).